






Developing a Spatially Explicit Humanitarian Flood Vulnerability Index for Refugee Settlements using Fuzzy Multi-Criteria Decision Analysis

Annika Kunz ¹, Ross S. Purves ¹, and Bruna Rohling ²

¹Department of Geography, University of Zurich, Switzerland

²Institute for Spatial and Landscape Development, ETH Zurich, Switzerland

Correspondence: Annika Kunz (annikakunz@me.com)

Abstract. The increasing number of refugees and the impacts of climate change necessitate improved flood vulnerability assessments for refugee settlements. Refugee settlements, often located in hazardous areas with limited infrastructure, tend to face high vulnerability. However, approaches to spatially assess flood vulnerability within these settlements are limited. This paper presents the development of a Humanitarian Flood Vulnerability Index (HFVI) tailored to refugee settlements, incorporating expert knowledge through the application of the Fuzzy Analytical Hierarchical Process (FAHP). The methodology takes into account the inclusion of expert judgment in weighting the indicators and integrates uncertainty analysis. A novel approach combines fuzzy logic with the One-at-a-Time (OAT) sensitivity method, providing a spatially explicit representation of weight uncertainties, to enable more informed decision-making and better-targeted interventions to ultimately improve the protection of refugees from flooding. The HFVI incorporates multiple vulnerability indicators, including physical and social dimensions, to create a composite raster-based index quantifying flood vulnerability in refugee settlements. A case study was performed in the UNHCR refugee settlement Mahama in Rwanda to illustrate the application of the HFVI using global and local data sets. The results demonstrate the effectiveness of the HFVI in identifying vulnerability hotspots. Limitations are discussed concerning the reproducibility and validity of the results, highlighting areas for improvement, ultimately aiming to enhance targeted flood risk mitigation strategies and resilience of refugee settlements to increasing flood risks.

Submission Type. Model, Case Study, Analysis

BoK Concepts. [GC1] Geocomputation and complex systems, [AM5] Basic analytical methods, [GS3] Use of geospatial information

Keywords. Flood Vulnerability Assessment, Refugee Settlements, Humanitarian Flood Vulnerability Index (HFVI), Fuzzy AHP, Weight Uncertainty

1 Introduction

Forced displacement and climate change as compounded global crises confront the most vulnerable populations with unprecedented challenges. By mid-2024, over 120 million individuals were forcibly displaced due to persecution, conflict, violence, and human rights violations. This number will grow in the coming years (UNHCR, 2024), while climate change will exacerbate natural hazards such as flooding (Seneviratne et al., 2021), disproportionately exposing marginalized communities with limited adaptive capacity to increased risks (Akola et al., 2019; Hassan et al., 2018; Malgwi et al., 2020).

Refugee settlements, often established as temporary solutions, frequently become long-term settlements where millions reside in precarious conditions (UNHCR, 2023). These settlements are highly vulnerable to floods due to their temporary infrastructure, which is exacerbated by socioeconomic vulnerabilities (Anwana and Owojori, 2023; Bernhofen et al., 2023; Rohling et al., 2023). Furthermore, the local political climate and land availability tend to influence the settlement location, often leading to the selection of remote and hazardous sites (ARSET, 2024). These areas are frequently overlooked in national top-down natural hazard assessments (Bernhofen et al., 2022, 2023).

Flood vulnerability, in combination with flood hazard, is integral to flood risk assessment (Nasiri et al., 2016), enabling decision-makers to reduce potential damage and fatalities (Chan et al., 2022; Fernandez et al., 2016). Vulnerability refers to the susceptibility of specific targets to damage in the event of a flood (Apel et al., 2008) and plays

a critical role in determining whether exposure will actually lead to a disaster (Ouma and Tateishi, 2014). Although the importance of flood risk assessments for refugee settlements has been stressed (Anwana and Owojori, 2023; Bernhofen et al., 2023; Mwalwimba et al., 2024), tailored approaches to spatially map vulnerability within refugee settlements do not exist. High-resolution data and modelling techniques used in existing frameworks are not easily applicable to refugee settlements, as they rely on data often not available in these settings (Akola et al., 2019; Anwana and Owojori, 2023; Hassan et al., 2018; Owen et al., 2023). Furthermore, those methodologies fail to address the settlements' physical and social vulnerabilities (Owen et al., 2023; Yi and Xie, 2010). Additionally, standardized methodologies addressing uncertainties are underutilized despite their potential to improve decision-making (An et al., 2022; Bernhofen et al., 2023). Incorporating expert knowledge can help mitigate data gaps and reflect the complex nature of vulnerability, while the integration of uncertainty analysis offers a deeper understanding of internal vulnerability factors (Bernhofen et al., 2023).

Recognizing these challenges, the UN refugee Agency (UNHCR), the Swiss Development Cooperation (SDC), and ETH Zurich initiated the "Sustainable Humanitarian Settlements" project through the Geneva Technical Hub (GTH) (UNHCR, n.d.) to enhance flood risk mitigation in refugee settlements by developing a GIS-based Risk Mitigation Strategy Tool. The tool integrates flood hazard and vulnerability assessments, enabling field staff to generate actionable risk maps (Gairing et al., 2024). This paper contributes to the project by proposing a Humanitarian Flood Vulnerability Index (HFVI), tailored to the context of refugee settlements. By incorporating multidimensional indicators, including physical and social vulnerabilities and expert-driven weighting, the HFVI addresses the limitations of existing flood vulnerability models. Additionally, the index employs sensitivity and uncertainty analyses to ensure robustness and transparency in decision-making.

2 Methods

2.1 Conceptual Index Development

The HFVI was developed to assess flood vulnerability in refugee settlements, focusing on social and physical vulnerability dimensions. To ensure reproducibility, the process followed the guidelines of the OECD and JRC's Handbook on Constructing Composite Indicators (JRC and OECD, 2008). Fig. 1 summarizes the steps taken to develop the HFVI and test its performance using geospatial data in a case study.

As a first step, eight indicators were selected based on an extensive literature review. Selection criteria (adopted from Birkmann and Pelling (2006)) included data avail-

ability, measurability and relevance to the refugee settlement conditions. The final set of social and physical vulnerability indicators is listed in Table 1.

2.1.1 Expert-Based Indicator Weight Calculation

Weighting of HFVI indicators relied on the Analytical Hierarchy Process (AHP), a multi-criteria decision analysis (MCDA) tool. AHP uses structured pairwise comparisons of criteria (C_i) to assign relative importance, systematically deriving weights for complex, multi-dimensional problems (Saaty, 1977).

A decision hierarchy was developed (Fig. 2), placing the overall flood vulnerability at the top (Level 0), followed by two dimensions - social and physical vulnerability (Level 1), and individual indicators at the lowest level (Level 2). Indicator weights were derived from questionnaires distributed to experts in flood and climate risk, humanitarian practitioners and related interdisciplinary fields. Eleven experts performed pairwise comparisons of the criteria C_i , here the selected indicators, assigning priority values (a_{ij}) reflecting the relative influence of each indicator on flood vulnerability within a general framework intended to be applicable to refugee settlements. A nine-point scale was used to set priorities, where 1 indicates equal importance and 9 indicates extreme importance (Saaty, 1980). Subsequently, priorities were transformed into pairwise comparison matrices (PCM) (Eq. 1) and weights were calculated by normalizing the PCMs, obtaining eigenvalues. Consistency was checked using the Consistency Ratio (CR), where a $CR \leq 0.1$ indicates acceptable judgments (Saaty, 1980). Inconsistent answers were transformed using Harker's algorithm (Harker, 1987). Strongly inconsistent answers were not included in further analysis.

$$PCM = \begin{matrix} & \begin{matrix} C_1 & C_2 & \cdots & C_n \end{matrix} \\ \begin{matrix} C_1 \\ C_2 \\ \vdots \\ C_n \end{matrix} & \begin{bmatrix} a_{11} & a_{12} & \cdots & a_{1n} \\ a_{21} & a_{22} & \cdots & a_{2n} \\ \vdots & \vdots & \ddots & \vdots \\ a_{n1} & a_{n2} & \cdots & a_{nn} \end{bmatrix} \end{matrix} \quad (1)$$

with $a_{ii} = 1, \quad a_{ji} = \frac{1}{a_{ij}}, \quad a_{ij} \neq 0$

2.1.2 Weight Uncertainty Incorporation

Given the inherent subjectivity and uncertainty of expert judgments the Fuzzy Analytical Hierarchy Process (FAHP) (Chang, 1996) was applied. Unlike traditional AHP, which relies on precise numerical judgments, FAHP uses Triangular Fuzzy Numbers (TFNs) to represent relative importance of criteria. TFNs are characterized by lower (l), modal (m) and upper bounds (u) and defined as a group of objects with an associated degree of membership between 0 and 1. The degree is described by a membership function (Eq. 2), expressing how strongly objects

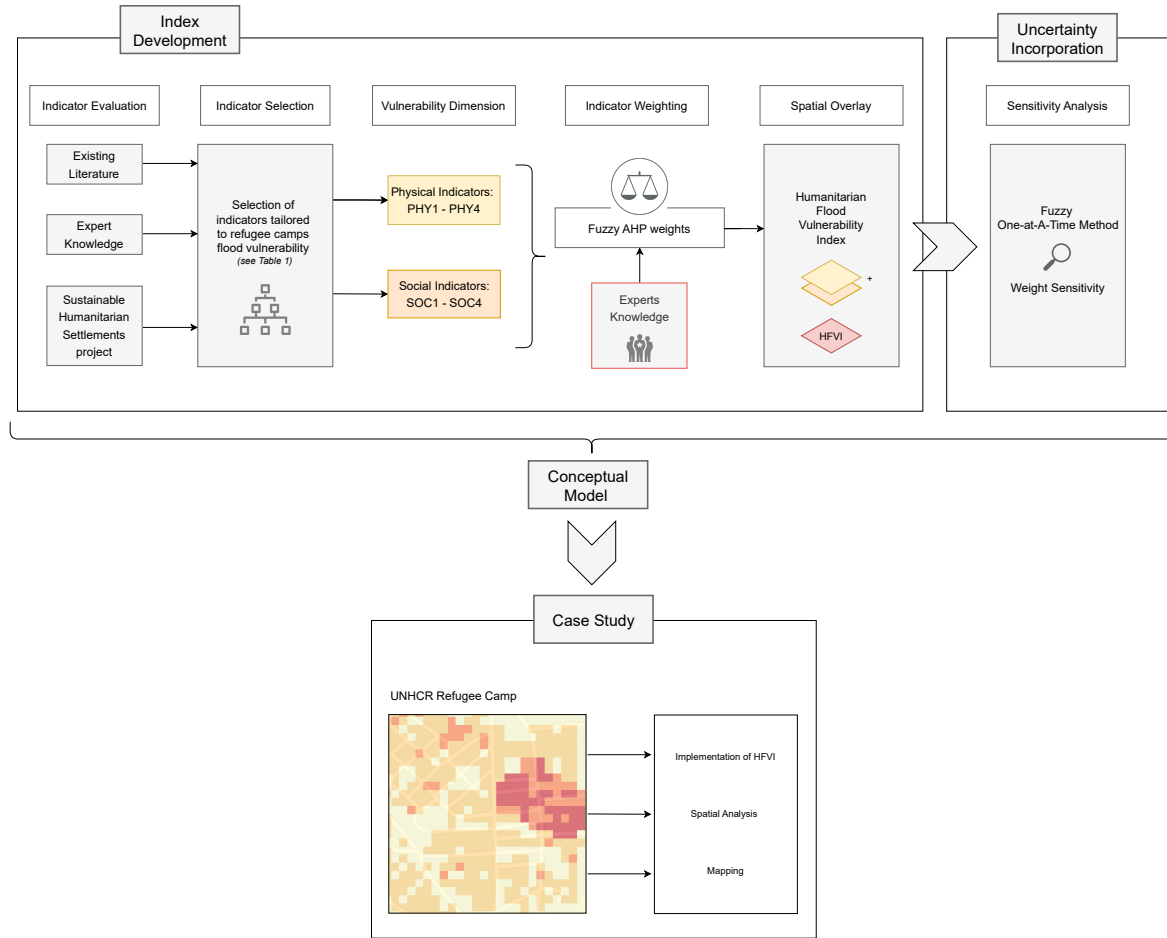


Figure 1. Graphical representation of the methodology, including the conceptual index development and the case study application.

belong to a set (Yang et al., 2013). For a TFN, the membership function is triangular, where l and u specify the interval fuzzy degree, while m depicts the most probable value (Ganji et al., 2022).

$$\mu_A(x) = \begin{cases} \frac{(x-l)}{m-l} & l \leq x \leq m \\ \frac{(x-u)}{m-u} & m \leq x \leq u \\ 0 & \text{otherwise} \end{cases} \quad (2)$$

FAHP was implemented by transforming crisp PCMs into fuzzy PCMs to derive fuzzy weights using Buckley's geometric mean method (Buckley, 1985). The fuzzy weights for each PCM were defuzzified using the arithmetic mean (Fozaie and Wahid, 2022) and normalized before being aggregated to produce the final indicator weights, enhancing the robustness of the weighting process by accommodating variability and imprecision in expert evaluations (Ganji et al., 2022).

2.1.3 Indicator Raster Calculation

After determining indicator weights, spatial data were prepared to allow the calculation of the HFVI. For each indi-

cator, an individual raster layer was created at a 30-meter resolution to capture spatial patterns within the settlement. Each raster cell was normalized to values between 0 and 1, representing counts, densities, or presence of elements depending on the indicator. For the quantitative indicator (SOC1), values were normalized and categorized into vulnerability classes. For the remaining categorical indicators, subcategories were assigned to predefined vulnerability ranks provided by Rohling et al. (2023) as given in Table 1. For each cell, the occurrence of each subcategory was multiplied by its rank, and a weighted sum was computed, producing normalized raster layers.

2.1.4 HFVI Calculation - Weighted Raster Overlay

The HFVI was constructed using a weighted linear combination of the normalized indicator layers multiplied by the derived FAHP weights using Eq. 3, where $w_{SOC_{dim}}$ and $w_{PHY_{dim}}$ are the FAHP weights for the social and physical dimensions, soc_i and phy_j are the raster layers for the i -th social and j -th physical indicator, $f_{w_soc_i}$ and $f_{w_phy_j}$ are their respective FAHP indicator weights,

Table 1. Final flood vulnerability indicator set including social and physical flood vulnerability dimensions and vulnerability ranks of indicators subcategories (0 = no vulnerability, 1 = low vulnerability, 2 = moderate vulnerability, 3 = high vulnerability).

Dim.	Abbr.	Indicator name	Description	Subcategory (Rank)	Geospatial Data	Scope
Social	SOC1	Population Density	Population density, calculated using average occupancy per shelter and shelter counts per raster cell	Equal intervals classification	Google Open Buildings Dataset (Sirko et al., 2021)	global
	SOC2	Vulnerable Groups	Presence of vulnerable groups	Presence of vulnerable groups (3), No presence of vulnerable groups (0)	PGIS mapping workshop with camp officers (Gairing et al., 2024)	local
	SOC3	Facilities of Social Importance	Counts of facility type per raster cell	Health Center (3), Nutrition Center (3), Security (3), Schools and ECD (2), Cultural Facilities (2), Youth/Women Center (2), Administrative Facilities (2), Distribution Center (2)	UNHCR camp site layout	local
	SOC4	Land Use	Land cover class of social importance	Agricultural Land (3), Open Space (2), Built-Up (0), Vegetation and Water (0)	Global Land Cover and Land Use (Potapov et al., 2022) or UNHCR camp site layout	global / local
Physical	PHY1	Shelter Type	Counts of residential shelter types per raster cell	Emergency Shelters (3), Transitional Shelters (2), Durable Shelters (1), Abandoned (0)	Google Open Buildings (Sirko et al., 2021) and PGIS mapping workshop with camp officers	global / local
	PHY2	Critical Infrastructure	Presence and type of critical infrastructure	Fragile Building Infrastructure (3), Sanitary Infrastructure (3), Water Tanks (3), Communication Infrastructure (3), Power Station Infrastructure (3), Drainage System (2)	PGIS mapping workshop with camp officers	local
	PHY3	Facilities Physical Vulnerability	Counts of facility type per raster cell	Cultural Facilities (3), Schools and ECD (2), Health Center (2), Youth/Women Center (2), Administrative Facilities (2), Security (2), Nutrition Center (2), Distribution Center (2)	UNHCR camp site layout	local
	PHY4	Roads	Frequency of road types per raster cell	Service Road (3), Bridge (3), Residential Road (2), Path (1), Footway (1), Unclassified (1)	Open Street Map Highways Dataset (OpenStreetMap contributors, 2017)	global

and n and m are the total numbers of social and physical indicators.

$$HFVI = wSOC_{dim} \times \left[\sum_{i=1}^n (soc_i \times f_w_soc_i) \right] + wPHY_{dim} \times \left[\sum_{j=1}^m (phy_j \times f_w_phy_j) \right], \quad (3)$$

2.2 Sensitivity Analysis

To evaluate the HFVI's sensitivity to indicator weights and identify areas of potential uncertainty, a sensitivity analysis was conducted using the One-At-a-Time (OAT)

method (Daniel, 1973) in combination with the FAHP. The weight of one indicator was systematically varied, while keeping others constant, observing the effects on the overall vulnerability map (Chen et al., 2010; Crosetto and Tarantola, 2001). The feasible range of weight changes, expressed as the Range of Percent Change (RPC) (Chen et al., 2010), was defined using the lower (w_l) and upper (w_u) bounds of the FAHP-derived fuzzy weights before defuzzification. Incremental weight adjustments of $\pm 1\%$ change within their RPC bounds were applied.

The weight of a modified indicator $W(c_m, pc)$ at a given percentage change (pc) was then calculated using Eq. 4, where $W(c_m, 0)$ represents the base weight of the main changing indicator c_m .

$$W(c_m, pc) = W(c_m, 0) + W(c_m, 0) \times pc, \quad (4)$$

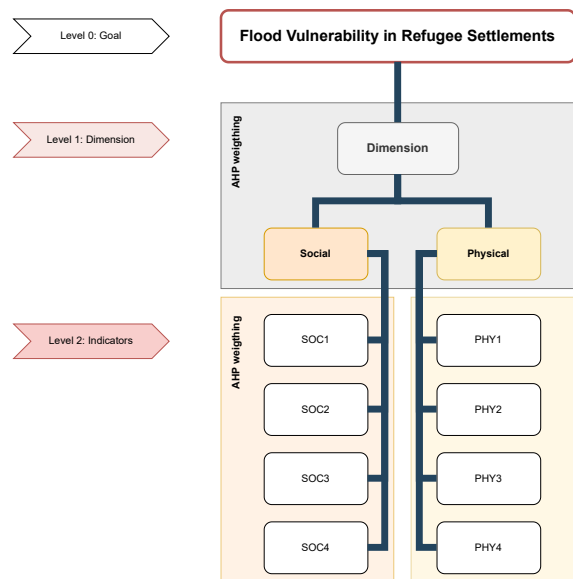


Figure 2. HFVI decision hierarchy and respective hierarchy levels, including social and physical vulnerability indicators.

The weights of the remaining indicators $W(c_i, pc)$ were proportionally modified to maintain the additivity constraint, ensuring the sum of the total weights was one, using Eq. 5:

$$W(c_i, pc) = \frac{(1 - W(c_m, pc)) \cdot W(c_i, 0)}{(1 - W(c_m, 0))}, \quad (5)$$

where $W(c_i, 0)$ is the weight of the i -th criterion c_i in the base run (Chen et al., 2010).

By varying weights across their RPC bounds, a series of evaluation maps were produced for each simulation run, quantifying spatial variability in HFVI outcomes due to weight changes (Chen et al., 2010). The simulation process was implemented using the SpatMCDA package in R (Wang et al., 2024). SpatMCDA is a toolset originally designed for spatial MCDA in data-scarce environments, generating maps of spatial uncertainty within the decision-making framework (Wang et al., 2024).

Incorporating fuzzy logic into the OAT methodology, our combined FAHP-OAT approach introduces a mechanism in spatial MCDA that captures uncertainty in weight assignments and addresses the subjectivity inherent in expert judgments.

2.3 Case Study Application

The HFVI was applied to the UNHCR Mahama refugee settlement in Rwanda to evaluate spatial patterns of flood vulnerability and test the performance of the developed HFVI. Mahama, the largest refugee settlement in Rwanda, is located in a flood-prone region due to its proximity to

the Kagera River, heavy rainfalls and inadequate drainage (UNHCR and MINEMA, 2023).

Geospatial data, including global datasets such as the Google Open Buildings Dataset (Sirko et al., 2021) and OpenStreetMap (OpenStreetMap contributors, 2017), as well as local data obtained from participatory mapping with camp officers, carried out by Kostenwein et al. (2023) and the camp layout provided by the UNHCR were utilized to compute the individual indicator raster layers for the case study application (see Table 1). The HFVI was calculated by overlaying these raster layers using the FAHP-derived weights and Eq. 3, producing a final composite vulnerability map. Accompanying the final HFVI map, social and physical vulnerability can also be assessed independently to allow an understanding of the underlying drivers of increased vulnerability. The resulting maps were analyzed to identify spatial patterns of flood vulnerability within the settlement. Further, FAHP-OAT sensitivity analysis using varying weight scenarios resulted in a final uncertainty map.

2.4 Data and Software Availability

The methodology was implemented using RStudio and ArcGIS Pro. Research data and code supporting this publication are available via the following repository [10.5281/zenodo.15176314](https://doi.org/10.5281/zenodo.15176314). The data record includes all scripts (AHP analysis, FAHP analysis, HFVI calculation), data and documentation necessary for the replication of the HFVI. Global datasets required for the spatial HFVI application can be downloaded for any area of interest as described in the README.md file provided. Sensitive local data used in the case study performed as part of this work (e.g. the location of vulnerable people within the settlement obtained from participatory mapping workshops) cannot be published for ethical reasons. However, to ensure reproducibility and to provide a practical example of the HFVI calculation using geospatial data, synthetic data was generated for a fictional refugee settlement to demonstrate the performance of the developed index. For a future application of the index to a given refugee settlement, effort should be spent on collecting data for those indicators that need local inputs (see Table 1). The synthetic local datasets, provided in the repository, can be used as templates for replication.

3 Results

3.1 Expert-Based Indicator Weights

The experts' pairwise comparisons provide insights into the relative importance of vulnerability indicators across the social and physical dimensions. Fig. 3 illustrates the distribution of individual weights derived from the AHP process. For social indicators, Population Density (SOC1) was consistently ranked most important, with a

median weight of 40.33%, followed by Vulnerable Groups (SOC2) at 26.22%. The least influential indicator, Land Use (SOC4), received a median weight of only 6.04%. However, the results highlight divergence in expert judgments, particularly for SOC1 and SOC2, as indicated by the wider range of weights. Physical indicators showed less variability in weights. Facilities Physical Vulnerability (PHY3) received the highest median weight of 33.12%, reflecting its critical role in flood vulnerability, while Shelter Type (PHY1) followed with 29.20%. Roads (PHY4) were ranked the least significant, with a median weight of 11.42%. The consistency among physical indicators underscores greater consensus among experts compared to the social dimension.

Fig. 3 also illustrates inconsistent PCMs (CR > 0.1) before applying Harker's method, emphasizing significant variability in expert judgments across both social and physical vulnerability indicators. The transformation process reduced inconsistency by 66.7% for social indicators and 60.0% for physical indicators. Among the indicators, Population Density (SOC1) and Vulnerable Groups (SOC2) exhibited the highest inconsistency for social indicators, while Shelter Type (PHY1) and Critical Infrastructure (PHY2) were the most inconsistent among physical indicators.

3.2 Final Fuzzy AHP Weights

The incorporation of fuzzy logic into the AHP process produced aggregated FAHP weights. Table 2 summarizes the final defuzzified weights and their fuzzy bounds. The results indicate the range of uncertainty in indicator prioritization. Among the social indicators, Population Density (SOC1) maintained the highest defuzzified weight of 39.7%, while Land Use (SOC4) remained the least influential with 7.9%. For physical indicators, Facilities Physical Vulnerability (PHY3) emerged as the most critical with 30.6%, followed by Shelter Type (PHY1) with 29.6%.

3.3 Spatial Pattern of the HFVI

The results of the case study application are based on the datasets described in Table 1 and enable the application of the developed HFVI to a real test case. The eight normalized raster layers represent the individual social and physical vulnerability indicators. The HFVI combines all indicators using Eq. 3 with the defuzzified expert weights by spatially overlaying the individual indicator raster layers. The final HFVI map in Fig. 4 highlights areas of varying flood vulnerability within the settlement, with values ranging from 0 (low vulnerability) to 1 (high vulnerability).

For the Mahama refugee settlement, clusters of high vulnerability are observed in regions driven by high Population Density (SOC1), the presence of Vulnerable Groups (SOC2), and Critical Infrastructure (PHY2). Moderately vulnerable areas coincide with mixed social and physical vulnerabilities, while the settlement's periphery shows

lower vulnerability due to the dominance of non-built-up areas. Spatial analysis confirms significant clustering in flood vulnerability, supported by Moran's I value of 0.632, indicating moderate positive spatial autocorrelation. Thus, the HFVI is effective in describing the relative spatial pattern of flood vulnerability on the settlement scale, highlighting vulnerable hotspots under increased flood risk.

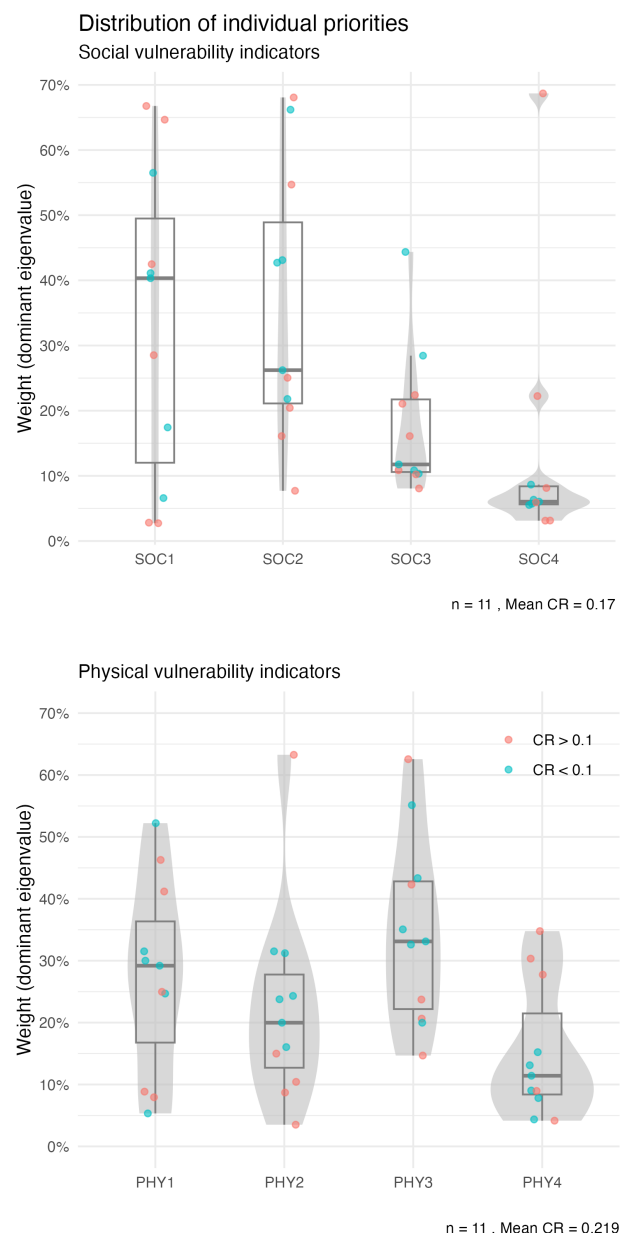


Figure 3. Distribution of individual priority weights per vulnerability indicator based on the AHP-questionnaire results using Saaty's eigenvalue method (Saaty, 2003). The jitter points represent the experts' priority weights and the Consistency Ratio (CR) value illustrates the consistency of the experts' answers before transformation, where CR > 0.1 represents inconsistency.

Table 2. Final FAHP weights.

Indicator	wMin	wModal	wMax	wDefuzzified	Vulnerability Dimension	Dimension Weight
SOC1	0.274	0.403	0.603	0.397	SOC	0.483
SOC2	0.223	0.339	0.525	0.337		
SOC3	0.117	0.184	0.301	0.187		
SOC4	0.044	0.074	0.137	0.079		
PHY1	0.151	0.295	0.570	0.296	PHY	0.517
PHY2	0.150	0.258	0.478	0.258		
PHY3	0.167	0.307	0.576	0.306		
PHY4	0.082	0.141	0.255	0.139		

3.4 HFVI Sensitivity

The sensitivity analysis, using the FAHP-OAT method, assessed the robustness of the HFVI by varying indicator weights within their fuzzy bounds. The results confirm that the HFVI remains stable under weight changes, with only minimal shifts in spatial patterns. Population Density (SOC1) and Shelter Type (PHY1) are the most weight-sensitive indicators, while Land Use (SOC4) and Roads (PHY4) exhibit the least sensitivity. Additionally, uncertainty maps were generated to visualize the impact of weight variability on the HFVI. Fig. 5 highlights the spatial pattern of uncertainty regions. High uncertainty regions coincide particularly with areas of high shelter concentrations and critical infrastructure.

4 Discussion

4.1 HFVI Conceptual Strengths and Limitations

The development of the Humanitarian Flood Vulnerability Index (HFVI) allows flood vulnerability assessment tailored to refugee settlements. It addresses a critical gap and provides a structured, spatially explicit methodology. The HFVI integrates multi-dimensional vulnerability indicators, combining social and physical dimensions into a composite raster-based index with a 30-meter resolution. This enables detailed spatial assessments and identification of vulnerability hotspots.

The HFVI methodology was explicitly designed for application in data-scarce environments, leveraging glob-

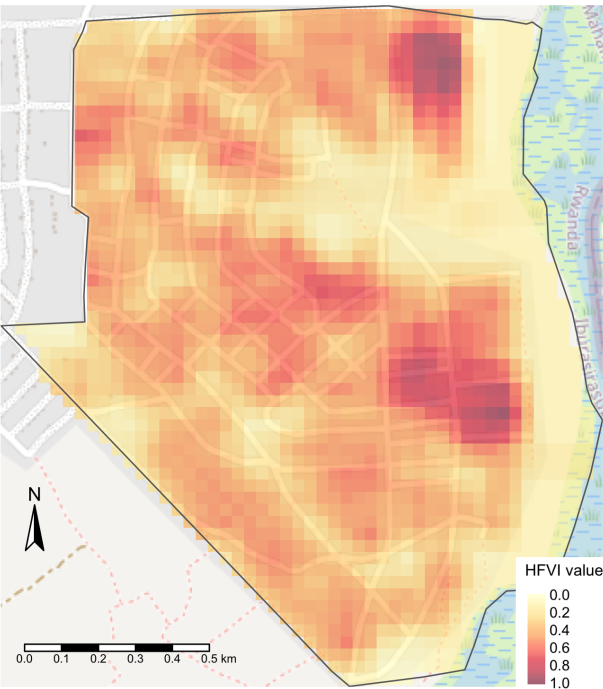


Figure 4. Final composite HFVI map, smoothed HFVI result using a low pass focal filter.

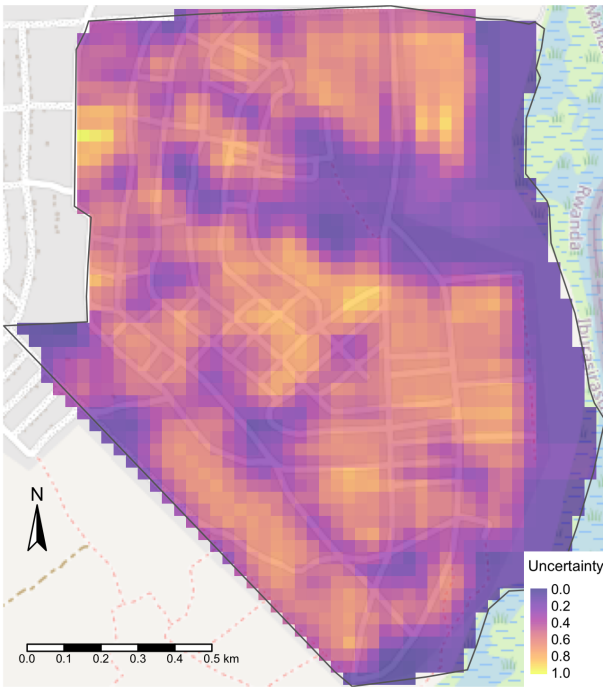


Figure 5. Final weight uncertainty map. Results are smoothed using a low-pass focal filter.

ally available datasets (Google Open Buildings, OpenStreetMap) and integrating local and participatory mapping to fill data gaps. While some indicators require localized inputs, such as Vulnerable Groups' locations (SOC2) or Facilities Physical Vulnerability (PHY3), these can be collected for future applications through low-resource participatory approaches, allowing applicability of the HFVI where high-resolution or empirical datasets are limited.

The HFVI leverages expert-derived weights, calculated using AHP and its fuzzy extension (FAHP), to provide a nuanced representation of indicator importance. The use of FAHP mitigates the relatively limited sample size by accommodating subjectivity and uncertainty in analyzing 11 expert judgments. The experts' diverse backgrounds introduced variability and potential bias, an inherent limitation of AHP, but also added interdisciplinary value, enriching the weighting process and reinforcing the case for using FAHP. Notably, indicators like Population Density (SOC1) and Vulnerable Groups (SOC2) showed higher inconsistencies, reflecting divergent expert opinions. These were partially addressed using Harker's method, highlighting the importance of explicitly incorporating uncertainty rather than disregarding it. The fuzzy weighting approach is thereby able to capture the complexity of vulnerability in refugee settlements. However, the exclusion of economic, environmental, and institutional dimensions, mainly due to data constraints, remains a key limitation to the comprehensiveness of the index.

4.2 HFVI Spatial Application and Performance

The application of the HFVI to the Mahama refugee settlement demonstrates the index's practicality in identifying spatial patterns of flood vulnerability. Vulnerability hotspots are identified in regions with high shelter density and population concentrations, where overlapping social and physical vulnerabilities contribute to elevated HFVI values. Key indicators such as Population Density (SOC1) and Shelter Type (PHY1) emerge as critical drivers of flood vulnerability. The incorporation of the FAHP-OAT sensitivity analysis further validates the robustness of the index, revealing that while certain indicators, like Land Use (SOC4) and Roads (PHY4), exhibit lower sensitivity, others like Population Density (SOC1) and Shelter Type (PHY1) show higher weight-sensitivity. The low sensitivity of Land Use (SOC4) and Roads (PHY4) can be attributed to their relatively low expert-assigned weights and narrower fuzzy weight ranges, reflecting expert consensus on their limited influence. Additionally, both indicators showed weaker spatial correlations with other vulnerability factors, reducing their impact on the composite HFVI when weights are varied. This finding underscores the importance of cautious interpretation of the results and the utility of uncertainty maps in supporting decision-making by highlighting spatial variability in vulnerability estimates and guiding the prioritization of interventions. By combining these maps with the HFVI results, decision-

makers can identify areas of high vulnerability coinciding with low uncertainty, enabling targeted mitigation strategies.

Despite its strengths, the HFVI is constrained by the data-scarce and dynamic nature of refugee settlements. The reliance on high-resolution global and local datasets introduces potential issues of data availability and accuracy in some regions of application. Additionally, the spatial resolution of 30 meters does not capture micro-scale variability in densely populated or highly heterogeneous areas. These constraints underscore the need for enhanced data collection and validation methods. While the HFVI is designed for transferability across varied geographic contexts, application to more case studies is needed to demonstrate its applicability in different settings. Validation was not performed due to data constraints, as ground-truth would require extensive fieldwork, data collection, and participatory workshops beyond this study's scope. These limitations highlight the need for future testing and validation across more diverse refugee settlement contexts to ensure the HFVI's broader applicability. In data-scarce settings, greater emphasis should be placed on participatory approaches involving local stakeholders, as shown in the Mahama case study, enabling the index's application despite limited data availability.

5 Conclusion and outlook

The HFVI represents a step forward in modelling flood vulnerability in refugee settlements by providing a quantitative, spatially explicit measure. The index's multi-dimensional approach, supported by expert knowledge and advanced sensitivity analysis, ensures a robust assessment of flood vulnerability. The HFVI, as a tool for the assessment of flood risks, lays the groundwork for more effective disaster preparedness and resilience in refugee settlements, while its integration into decision-making processes could support more targeted interventions.

The HFVI has potential for broader applications in flood risk management in refugee settlements. Integration into GIS-based tools, such as the UNHCR's Risk Mitigation Strategy Tool by Gairing et al. (2024), could enhance its usability, allowing field staff to generate actionable risk maps for any settlement. Validating the HFVI using additional refugee settlements with diverse geographic and socio-economic contexts, however, is crucial for guaranteeing its broader applicability. Testing the HFVI alongside hazard-specific datasets in flood risk models will allow for a more holistic approach to flood risk assessment, eventually seeking to enhance the living conditions in refugee settlements.

Acknowledgements

Author contributions. This study originated from AK's Master's thesis, who conducted the research, developed the methodology, performed data analysis, and wrote the manuscript. RSP and BR supervised the study, provided guidance on the research design and methods, and edited and reviewed the manuscript. All authors reviewed and approved the final manuscript. The authors gratefully acknowledge the valuable input of the 11 experts who contributed to the indicator weighting process through their participation in the AHP survey.

Disclaimer. The authors declare that they occasionally have used Generative AI tools in the preparation of this manuscript for language editing, improving grammar, and sentence structure, but not for generating scientific content, research data, or substantive conclusions. All intellectual and creative work, including the analysis and interpretation of data, is original and has been conducted by the authors themselves.

Competing interests. The authors declare that they have no competing interests.

References

- Akola, J., Binala, J., and Ochwo, J.: Guiding developments in flood-prone areas: Challenges and opportunities in Dire Dawa city, Ethiopia, *Jàmá Journal of Disaster Risk Studies*, 11, <https://doi.org/10.4102/jamba.v11i3.704>, 2019.
- An, T. T., Izuru, S., Narumasa, T., Raghavan, V., Hanh, L. N., An, N. V., Long, N. V., Thuy, N. T., and Minh, T. P.: Flood vulnerability assessment at the local scale using remote sensing and GIS techniques: A case study in Da Nang City, Vietnam, *Journal of Water and Climate Change*, 13, 3217–3238, <https://doi.org/10.2166/wcc.2022.029>, 2022.
- Anwana, E. O. and Owojori, O. M.: Analysis of Flooding Vulnerability in Informal Settlements Literature: Mapping and Research Agenda, *Social Sciences*, 12, <https://doi.org/10.3390/socsci12010040>, 2023.
- Apel, H., Merz, B., and Thielen, A. H.: Quantification of uncertainties in flood risk assessments, *International Journal of River Basin Management*, 6, 149–162, <https://doi.org/10.1080/15715124.2008.9635344>, 2008.
- ARSET: Earth Observations for Humanitarian Applications. NASA Applied Remote Sensing Training Program (ARSET), available at: <http://appliedsciences.nasa.gov/get-involved/training/english/arset-earth-observations-humanitarian-applications>, last access: 26.12.2024, 2024.
- Bernhofen, M. V., Cooper, S., Trigg, M., Mdee, A., Carr, A., Bhawe, A., Solano-Correa, Y. T., Pencue-Fierro, E. L., Teferi, E., Haile, A. T., Yusop, Z., Alias, N. E., Sa'adi, Z., Ramzan, M. A. B., Dhanya, C. T., and Shukla, P.: The role of global data sets for riverine flood risk management at national scales, *Water Resources Research*, 58, <https://doi.org/10.1029/2021WR031555>, 2022.
- Bernhofen, M. V., Blenkin, F., and Trigg, M.: Unknown risk: Assessing refugee camp flood risk in Ethiopia, *Environmental Research Letters*, 18, <https://doi.org/10.1088/1748-9326/acd8d0>, 2023.
- Birkmann, J. and Pelling, M.: Measuring vulnerability to natural hazards: Towards disaster resilient societies, United Nations University, 2006.
- Buckley, J.: Fuzzy hierarchical analysis, *Fuzzy Sets and Systems*, 17, 233–247, [https://doi.org/10.1016/0165-0114\(85\)90090-9](https://doi.org/10.1016/0165-0114(85)90090-9), 1985.
- Chan, S. W., Abid, S. K., Sulaiman, N., Nazir, U., and Azam, K.: A systematic review of the flood vulnerability using geographic information system, *Heliyon*, 8, <https://doi.org/10.1016/j.heliyon.2022.e09075>, 2022.
- Chang, D.-Y.: Applications of the extent analysis method on fuzzy AHP, *European Journal of Operational Research*, 95, 649–655, [https://doi.org/10.1016/0377-2217\(95\)00300-2](https://doi.org/10.1016/0377-2217(95)00300-2), 1996.
- Chen, Y., Yu, J., and Khan, S.: Spatial sensitivity analysis of multi-criteria weights in GIS-based land suitability evaluation, *Environmental Modelling and Software*, 25, 1582–1591, <https://doi.org/10.1016/j.envsoft.2010.06.001>, 2010.
- Crosetto, M. and Tarantola, S.: Uncertainty and sensitivity analysis: Tools for GIS-based model implementation, *International Journal of Geographical Information Science*, 15, 415–437, <https://doi.org/10.1080/13658810110053125>, 2001.
- Daniel, C.: One-at-a-Time Plans, *Journal of the American Statistical Association*, 68, 353–360, <https://doi.org/10.1080/01621459.1973.10482433>, 1973.
- Fernandez, P., Mourato, S., Moreira, M., and Pereira, L.: A new approach for computing a flood vulnerability index using cluster analysis, *Physics and Chemistry of the Earth*, 94, 47–55, <https://doi.org/10.1016/j.pce.2016.04.003>, 2016.
- Fozaie, M. T. A. and Wahid, H.: A guide to integrating expert opinion and Fuzzy AHP when generating weights for composite indices, *Advances in Fuzzy Systems*, 2022, 3396 862, <https://doi.org/10.1155/2022/3396862>, 2022.
- Gairing, M., Schalbetter, L., Antenen, N., Kostenwein, D., Rohling, B., Schmid, E., Nimri, R., Kaufmann, D., and Grêt-Regamey, A.: User Manual for the Risk Mitigation Strategy Tool in QGIS. General Manual, available at: https://www.humanitarian-risk.org/images/pdf/learning-section/02_Risk_Mitigation_Tool_Manual_-_General.pdf, ETH Zurich, UNHCR, 2024.
- Ganji, K., Gharechelou, S., Ahmadi, A., and Johnson, B. A.: Riverine flood vulnerability assessment and zoning using geospatial data and MCDA method in Aq'Qala, *International Journal of Disaster Risk Reduction*, 82, 103 345, <https://doi.org/10.1016/j.ijdrr.2022.103345>, 2022.
- Harker, P. T.: Derivatives of the Perron root of a positive reciprocal matrix: With application to the analytic hierarchy process, *Applied Mathematics and Computation*, 22, 217–232, [https://doi.org/10.1016/0096-3003\(87\)90043-9](https://doi.org/10.1016/0096-3003(87)90043-9), 1987.
- Hassan, M. M., Smith, A. C., Walker, K., Rahman, M., and Southworth, J.: Rohingya refugee crisis and forest cover change in Teknaf, Bangladesh, *Remote Sensing*, 10, 689, <https://doi.org/10.3390/rs10050689>, 2018.

- JRC and OECD: Handbook on constructing composite indicators: Methodology and user guide, European Union and Joint Research Centre, <https://doi.org/10.1787/9789264043466-en>, 2008.
- Kostenwein, D., Antenen, N., Rohling, B., Garining, M., E., S., Nimri, R., and Kaufmann, D.: Local Data Collection Guide, available at: https://www.humanitarian-risk.org/images/pdf/learning_section/04_Local_Data_Collection_Guide_with_Annex.pdf, ETH Zurich, UNHCR, Geneva Technical Hub, 2023.
- Malgwi, M. B., Fuchs, S., and Keiler, M.: A generic physical vulnerability model for floods: Review and concept for data-scarce regions, *Natural Hazards and Earth System Sciences*, 20, 2067–2090, <https://doi.org/10.5194/nhess-20-2067-2020>, 2020.
- Mwalwimba, I. K., Manda, M., and Ngongondo, C.: Flood vulnerability assessment in rural and urban informal settlements: Case study of Karonga district and Lilongwe city in Malawi, *Natural Hazards*, <https://doi.org/10.1007/s11069-024-06601-5>, 2024.
- Nasiri, H., Yusof, M., and Ali, T.: An overview to flood vulnerability assessment methods, *Sustainable Water Resources Management*, 2, 331–336, <https://doi.org/10.1007/s40899-016-0051-x>, 2016.
- OpenStreetMap contributors: Planet dump retrieved from <https://planet.osm.org>, <https://www.openstreetmap.org>, 2017.
- Ouma, Y. O. and Tateishi, R.: Urban flood vulnerability and risk mapping using integrated multi-parametric AHP and GIS: Methodological overview and case study assessment, *Water (Switzerland)*, 6, 1515–1545, <https://doi.org/10.3390/w6061515>, 2014.
- Owen, M., Kruczkiewicz, A., and Hoek, J. V. D.: Indexing climatic and environmental exposure of refugee camps with a case study in East Africa, *Scientific Reports*, 13, <https://doi.org/10.1038/s41598-023-31140-7>, 2023.
- Potapov, P., Hansen, M. C., Pickens, A., Hernandez-Serna, A., Tyukavina, A., Turubanova, S., Zalles, V., Li, X., Khan, A., Stolle, F., and Harris, N.: The global 2000–2020 land cover and land use change dataset derived from the Landsat archive: first results, <https://doi.org/10.3389/frsen.2022.856903>, 2022.
- Rohling, B., Kostenwein, D., Gairing, M., Kaufmann, D., Al-Mahdawi, A., Schmid, E., and Bardou, E.: Flood Risk in Humanitarian Settlements: Compendium of Mitigation Measures, ETH Zurich, UNHCR, <https://doi.org/10.3929/ethz-b-000645680>, 2023.
- Saaty, T.: A scaling method for priorities in hierarchical structures, *Journal of Mathematical Psychology*, 15, 234–281, [https://doi.org/10.1016/0022-2496\(77\)90033-5](https://doi.org/10.1016/0022-2496(77)90033-5), 1977.
- Saaty, T.: *The Analytic Hierarchy Process*, McGraw-Hill, 1980.
- Seneviratne, S., Zhang, X., Adnan, M., Badi, W., Dereczynski, C., Di Luca, A., Ghosh, S., Iskandar, I., Kossin, J., Lewis, S., Otto, F., Pinto, I., Satoh, M., Vicente-Serrano, S., Wehner, M., and Zhou, B.: Weather and climate extreme events in a changing climate, p. 1513–1766, Cambridge University Press, Cambridge, United Kingdom and New York, NY, USA, <https://doi.org/10.1017/9781009157896.013>, 2021.
- Sirko, W., Kashubin, S., Ritter, M., Annkah, A., Bouchareb, Y. S. E., Dauphin, Y., Keyzers, D., Neumann, M., Cisse, M., and Quinn, J.: Continental-Scale Building Detection from High Resolution Satellite Imagery, *arXiv*, <https://doi.org/10.48550/arXiv.2107.12283>, 2021.
- UNHCR: Refugee Camps, available at: <https://www.unrefugees.org/refugee-facts/camps/>, last access: 30 January 2025, 2023.
- UNHCR: Mid-Year Trends 2024, available at: <https://www.unhcr.org/mid-year-trends-report-2024>, last access: 07 February 2025, 2024.
- UNHCR: Climate change and displacement: Geneva Technical Hub, available at: <https://www.unhcr.org/what-we-do/build-better-futures/climate-change-and-displacement/geneva-technical-hub>, last access: 06. February 2025, n.d.
- UNHCR and MINEMA: Mahama Refugee Camp Factsheet September 2023: United Nations High Commissioner for Refugees and Ministry of Emergency Management, available at: <https://data.unhcr.org/en/documents/details/96735>, last access: 07 February 2025, 2023.
- Wang, H., Zeng, J., Liu, T., Gao, X., Hongbin, W., and Jianhua, X.: SpatMCDA: An R package for assessing areas at risk of infectious diseases based on spatial multi-criteria decision analysis, <https://doi.org/10.5281/zenodo.11044224>, 2024.
- Yang, X., Ding, J., and Hou, H.: Application of a triangular fuzzy AHP approach for flood risk evaluation and response measures analysis, *Natural Hazards*, 68, 657–674, <https://doi.org/10.1007/s11069-013-0642-x>, 2013.
- Yi, S. and Xie, Y.: Vulnerability analysis of disaster risk based on geographic information and Dempster-Shafer theory, in: 18th International Conference on Geoinformatics, pp. 1–6, <https://doi.org/10.1109/geoinformatics.2010.5567898>, 2010.